



ARTICLE

Cellular Automata Simulations of Random Pitting Process on Steel Reinforcement Surface

Ying Wang*, Haoran Shi and Shibo Ren

Jiangsu Key Laboratory of Engineering Mechanics, Southeast University, Nanjing, 211189, China

*Corresponding Author: Ying Wang. Email: civil_wangying@seu.edu.cn

Received: 14 January 2021 Accepted: 17 May 2021

ABSTRACT

The corrosion of reinforcement in the concrete will cause the effective cross-sectional area of reinforcement to be weakened and the performance of reinforcement to change and lead to the degradation of the bond behavior between reinforcement and concrete, which can seriously affect the mechanical properties of the structural elements. Therefore, it is of great practical significance to accurately simulate the corrosion morphology and the corrosion products of reinforcement. This paper improves the previous cellular automata models and establishes a new cellular automata model framework for simulating the random pitting corrosion process of reinforcement in concrete. This model defines the detailed local evolution laws of material transformation, penetration and diffusion processes during the corrosion. Meanwhile, based on the spatial inhomogeneity of corrosion, three parameters are introduced into the model: The dissolution probability parameter p , the local corrosion space parameter λ and the local corrosion probability parameter ε , which establishes a parameterized model of corrosion probability. The research results show that the common steel reinforcement corrosion morphology can be obtained by adjusting the parameters. The volume expansion rate of the corrosion products is about 2, which is consistent with the relevant experimental research results. The cellular automata model in this paper can simulate the common steel reinforcement corrosion morphology and corrosion products in engineering.

KEYWORDS

Corrosion of reinforcement; cellular automata; simulation; corrosion morphology

1 Introduction

Relevant studies have shown that, in the alkaline environment, a layer of dense passive film about 10 nm thick will be generated on the surface of the reinforcement in the concrete structure to protect the reinforcement from corrosion [1]. In the process of structural service, the working environment of reinforcement is changed due to the combined action of many factors such as carbonation and chloride penetration. The passive film originally generated in alkaline medium is destroyed and the reinforcement loses its protection. The corrosion caused by carbonation usually appears as uniform corrosion, and the corrosion caused by chloride penetration usually appears as pitting corrosion. In practical engineering, most corrosion of reinforcement is related to chloride penetration, and the volume of corrosion products is two to three times or more of



the volume of corroded metal, which causes the concrete cover to crack longitudinally along the steel reinforcement [2]. Once cracks occur, the corrosion rate of steel reinforcement will be greatly accelerated. Reference [3] summarized the influence of steel corrosion on reinforced concrete structural performance in chloride ion environment. On the one hand, the local corrosion on steel reinforcement surface can weaken the section of steel reinforcement, cause stress concentration and reduce the mechanical properties of steel reinforcement. On the other hand, cracking due to corrosion expansion can reduce the grip force between steel reinforcement and concrete. Severe loss of rib height by corrosion can reduce the mechanical bite force. Also, the thicker corrosion product on steel/concrete interface which can be regard as a lubrication will further degrade the bonding performance. Combine these two factors, steel reinforcement corrosion in chloride ion environment can decrease concrete durability and structural bearing capacity and increase the possibility of brittle failure of structure. Therefore, it is very necessary to accurately simulate the corrosion morphology and corrosion products of reinforcement in concrete.

Most studies on the performance of corroded metal components have pre-defined the shape of pitting pits, many scholars used geometric figures to simulate the morphology. Val et al. [4] were first to propose the hypothesis of hemispherical shape to describe the section shape of pitting pits and calculated the section area of steel reinforcement after local corrosion in 1997. Since then, the hemispheric hypothesis has been adopted in many mechanical property degradation analyses of members with pitting corrosion [5,6]. Based on the hemispherical, Shen et al. [7] proposed the hypothesis of semi-ellipsoid hypothesis which assumed that the long axis of ellipsoid was along the axis of the steel reinforcement, and the center of ellipsoid was always on the circumference of the cross-section. In fact, due to the characteristics of metal materials and the influence of complex environmental factors, the corrosion morphology is not a hemispherical or regular semi-ellipsoidal shape. Wang et al. [8,9] observed and counted the pitting pit morphology of many steel reinforcement surfaces. According to the length, width and depth of pitting pits, the macro pits were classified into two categories: deep narrow type and open type, including deep ellipsoid, spherical, long ellipsoid and groove. Xu [10] observed of the section morphology of 73 pitting pits and classified the pits into two types: wide and shallow type and narrow and deep type. Wang et al. [11] built virtual models of corroded steel reinforcement by using 3D laser scanning technology and screened 693 severely corroded sections. The observation results of the residual section showed that corrosion type of steel reinforcement in carbonization environment is mainly uniform corrosion, while the pitting pit in chloride erosion environment develops significantly, and the shape of pitting corrosion pit can be divided into oval shape, wide shallow shape and undercut shape. Fig. 1 shows the typical morphology of pitting pits on steel reinforcement surface obtained through the above experiments.

As the corrosion environment of steel reinforcement is very complex, it is difficult to keep the corrosion simulation consistent with the real corrosion situation. The corrosion morphology of steel reinforcement is difficult to be accurately predicted. Therefore, a more practical calculation model is needed, which can predict the growth process of pits and reflect the morphology of pits. Cellular Automaton (CA) technology has been used in many areas of material science in recent years, especially in the field of corrosion science. CA technology has powerful functions. It can be used to model at the microscopic or mesoscopic level and map the reaction results at the microscopic or mesoscopic level to the macroscopic level. Different from traditional dynamic methods, CA does not rely on fixed physical equations and functions but is composed of a series of rules constructed by models [12]. Therefore, it can be used as an effective tool for the study of complex systems.

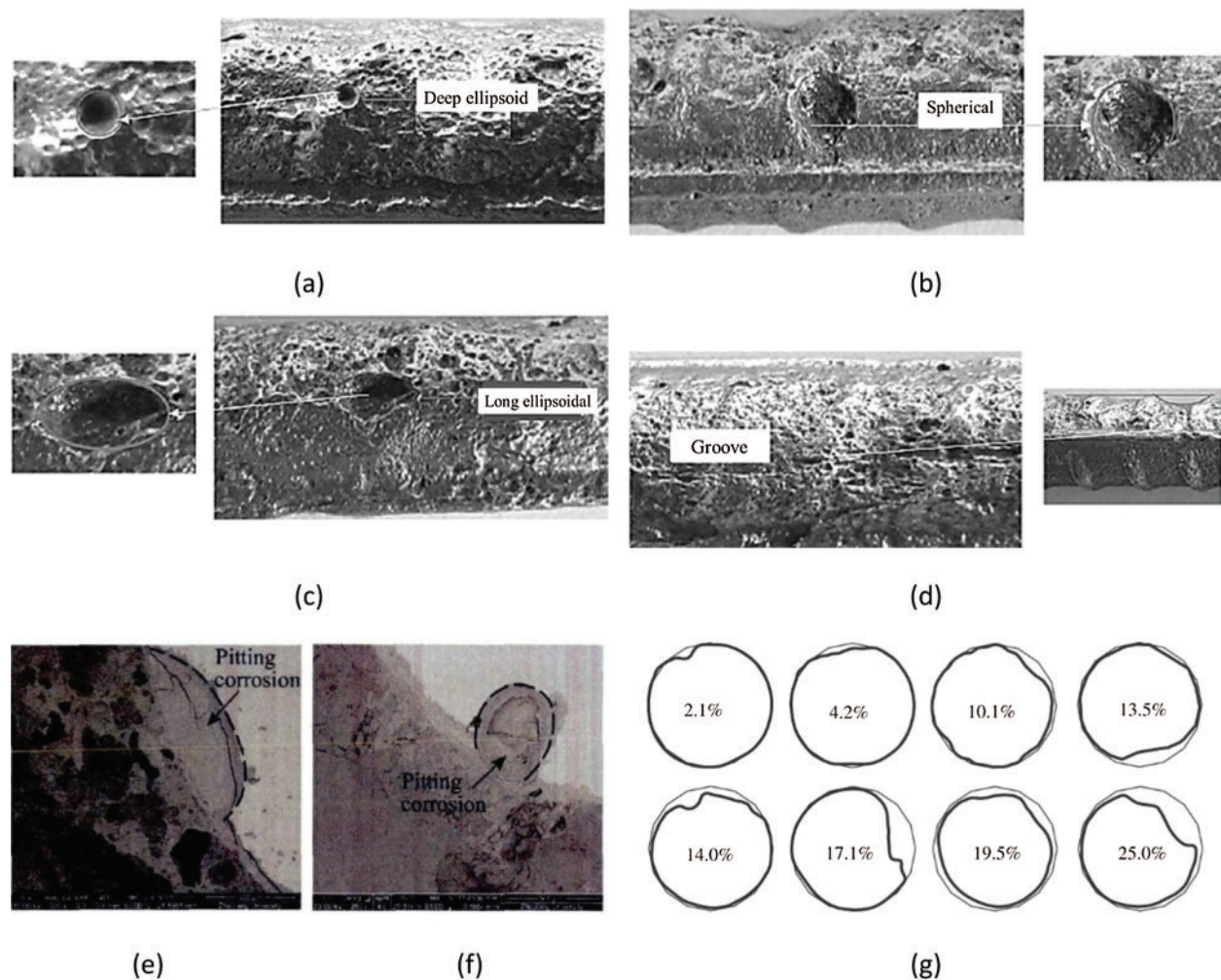


Figure 1: Measured morphology of pitting pits on steel reinforcement surface: (a)–(d): four typical corrosion pits observed by Wang et al. [8] ((a): deep ellipsoid, (b): spherical, (c): long ellipsoid, (d): groove), (e)–(f): morphology of corrosion pits observed by Xu [10] ((e): wide and shallow, (f): narrow and deep), (g): section shape of steel reinforcement under different mass loss rates in chloride salt environment [11]

CA corrosion models usually use probabilistic events instead of electrochemical reaction constants to reflect corrosion behavior. The early CA corrosion models have relatively simple cell types and local evolution rules. Cordoba-Torres et al. [13] were the first to use CA technology to study corrosion mechanism. They established a two-dimensional probabilistic CA corrosion model and determined a set of evolution rules of anodic dissolution based on the Von. Neumann type neighbor and obtained rough corrosion surface under random electrochemical behavior. Metal electrodes are no longer regarded as indivisible units, but as a collection of independent units in the form of cells. Malki et al. [14] used the linear function of dissolution probability to characterize the transition law of IR drop in corrosion pits and studied the dissolution probability and its influence on the growth and morphology of corrosion pits by establishing a two-dimensional CA model. The results showed that dissolution probability strongly affected the morphology and tn law of pitting corrosion. Bartosik et al. [15] made an in-depth study on corrosion damage

and passivation of metal materials by using CA. Pidaparti et al. [16] used probabilistic CA to simulate the pitting corrosion of aluminum alloy in aerospace materials and determined the evolutionary rules of the occurrence and development of pitting corrosion with the Von. Neumann neighbor. Stafiej et al. [17] made an in-depth study of corrosion damage and passivation on metal materials by using CA and analyzed the roughness of corrosion damage morphology. Li et al. [18] established the evolution rules of CA model based on the mechanism the results of the early corrosion test of metals in humid atmosphere, and simulated the electrochemical reaction and diffusion process in the process of metal corrosion. Wang et al. [19] used the number of dissolved cells in the simulation process to represent the dissolution current, and used the number of dissolved cells in the two-dimensional cellular automata grid to represent the depth of erosion pit, and studied the variation of dissolution current with time under different conditions. Liu [20] used CA to simulate the corrosion phenomena of metal, such as single point corrosion, multi-point corrosion, single slit corrosion and multi-slit corrosion. However, there were few cell types in the model, and the parametrized modeling of corrosion rate based on local corrosion characteristics was not considered, so the model only realized simple simulation of corrosion.

In the local corrosion model established by Caprio et al. [21], parameterized definitions of corrosion probability were introduced, including dissolution probability parameters, spatial parameters and local corrosion probability parameters, which realized the spatial heterogeneity of local corrosion and obtained different corrosion morphology easily by changing the parameters. He et al. [12] established the framework of two-dimensional CA local corrosion, defines the local evolution rules for transformation, infiltration and diffusion in metal corrosion process. The complex simulation of local corrosion on metal surface with and without protective coating is realized. A variety of common pitting pits were obtained by adjusting the parameters, and the influence of different parameters on the corrosion depth was explored. However, the results of the pitting corrosion simulation above cannot obtain the corrosion products with enough volume expansion, which cannot be well used in the study of the pitting corrosion of steel rebars. The volume expansion rate of corrosion products is an important parameter in the analysis of failure of reinforced concrete due to corrosion expansion. The value range of volume expansion rate in different models is 2~3. Volume expansion rate in the cracking model of corroded reinforced concrete established by Molina et al. [22] is 2. Ji et al. [23] used X-ray diffraction technology to analyze the expansion properties of corrosion products under different corrosion conditions and degrees. The expansion ratios of corrosion products under different corrosion conditions were close, about 2.20~2.45.

In conclusion, the existing corrosion CA models are all oriented to the corrosion dissolution process and the morphology evolution and volume expansion of the corrosion products during the corrosion process is not considered enough. The corrosion expansive force of reinforcement is closely related to the morphology of corrosion products. The existing research adopt the simplified equivalent load inside the concrete to simulate the cracking due to corrosion expansion, which cannot reflect the corrosive products in the process of corrosion morphology of irregularity and will reduce the adverse effect of the corrosion expansive force.

In this paper, we have improved the local evolution rules in CA model which can obtain both the corrosion morphology and corrosion product morphology. Based on previous research content, a CA model frame is established to study the corrosion of steel reinforcement in concrete. The model discretizes the metal and solution into ordered cells in the CA system and defines the relatively strict local evolution rules. Meanwhile, the model introduces the corrosion probability of parameterized definition. Thus, the corrosion morphology under different condition and

the influence law of different parameters on the corrosion process is concluded. The complex simulation of the process of metal dissolution and corrosive products generate on mesoscopic scale is realized.

2 Cellular Automata Model of Random Pitting

2.1 Definition and Composition of Cellular Automata

CA is a mesh dynamic model which is discrete in time, space and state. It takes spatial interaction and temporal causality as local rules. It can simulate the complex spatiotemporal evolution process. The mathematical definition of CA is relatively strict, which is called deterministic CA, and its evolution rule is a definite mapping relation. But the corrosion process is uncertain, so the local evolution rule needs to introduce probability rule to realize the corrosion simulation process.

As shown in Fig. 2, the basic elements of CA include cellular, cellular state, cellular space, neighbor cellular, discrete time set and local evolution rules. There may be many types of cells in a CA model, which is the most basic element in the CA and the basic unit participating in the evolution. Each cell has a specific cellular state in each discrete time increment, and the set of spatial positions occupied by all cells according to the established distribution law constitutes the cellular space of the model. CA can describe and evolve the dynamic characteristics of the system by changing the state value of the cell according to local rules in each discrete time increment. The state of cells at each moment is related to the state of itself and its neighbor cell.

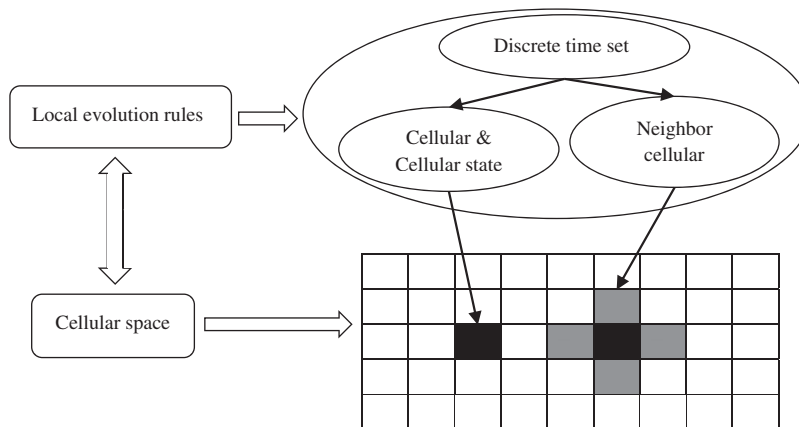


Figure 2: The composition of cellular automata [24]

2.2 Physical Model

The corrosion of steel reinforcement in concrete will occur under chloride penetration, and the pitting process of steel reinforcement is an electrochemical reaction process. The anodic reaction of electrochemical reaction is the dissolution reaction of metal, while the cathodic reaction is the reduction reaction of oxygen. The expression is as follows:

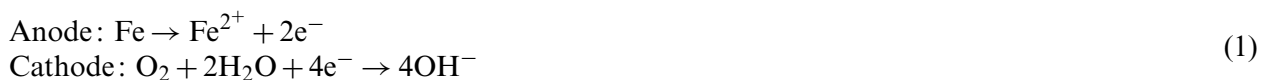


Fig. 3 is a schematic diagram of metal pitting. The composition of corrosive products after the metal pitting is complicated, mainly including the incomplete oxidation of ferrous iron compounds and completely oxidized ferric iron compounds. The composition of corrosion products

will not be specifically discussed in this paper, it is collectively referred to as the corrosion products. The corrosion products and their morphology will be reflected in the following simulation results.

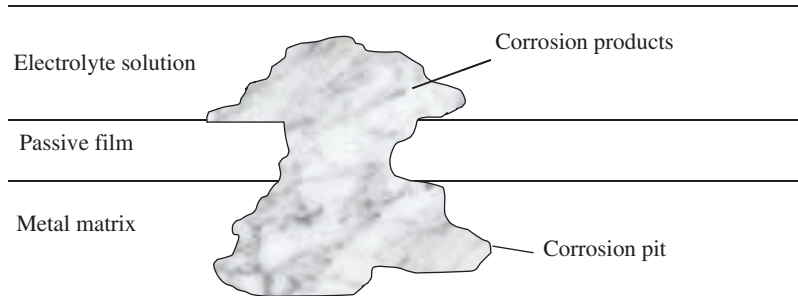


Figure 3: Pitting corrosion of metal

2.3 Definition of Cellular Space

Corrosion of reinforcement is one of the more complex physical and chemical process. Based on the purpose of this study, we focus on pitting corrosion morphology and generation of corrosion products. Therefore, necessary simplifications are made to the model. The corrosion model does not take into account of various soluble pollutants in electrolyte solution, such as temperature, pH and salinity (chloride, sulfate ion, etc.). The model does not simulate a single one of these factors but will consider these factors as the initial corrosion liquid and control the corrosion process by controlling the mass loss rate ($\omega = \text{cell number of dissolved metal}/\text{initial metal cellular number}$).

In this paper, the corrosion system is discretized into a two-dimensional space with the size of 100×50 . The neighbor cellular type used in the CA model is Von. Neumann (four-neighbor cell) type. And periodic boundary conditions are selected to simulate the relatively infinite space under the ideal state. The initialization of cellular space is shown in Fig. 4. The upper half (lines 1–50) of cellular space is the corrosive solution cell, the lower half (lines 52–100) is the metal cell, and the surface of the metal cell (line 51) is the metal passive film.

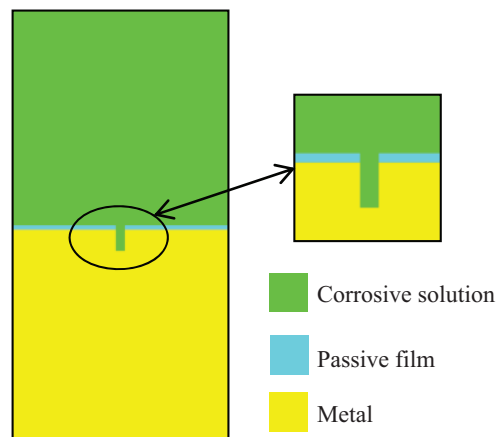






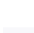
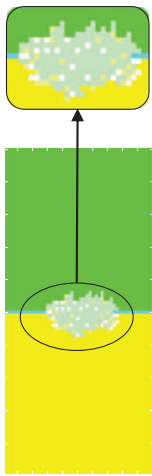


Figure 4: Initial state of cellular space

Through the microscopic observation of the interface between concrete and different corrosion stages, it is found that before the concrete cover cracks, the corrosion mainly occurs on the side near the concrete cover. The pitting pit density decreases with the increase of the distance between reinforcement surface and concrete cover [25]. Therefore, an initial defect was set in the middle of the passive film to simulate the damage point in the area near the concrete cover of the reinforcement. The initial defect was filled with corrosive solution, and its transverse size was 1% of the whole cellular space transverse size. The CA model established in this paper involves a total of 7 cell types, whose symbols, names, meanings and other information as well as the schematic diagram of corrosion products are shown in Tab. 1.

Table 1: Type and meaning of cells

Symbol	Name	Meaning	Color
B	Passive film cell	Passive film	
M	Metal cell	Metal	
S	Corrosive cell	Corrosive solution	
L	Corrosion products cell	Corrosion products	
D	Intermediate cell	Diffusate	
LS	Composite cell -1	The corrosion solution exists in the voids of the corrosion products	
LD	Composite cell -2	The diffusate exists in the voids of the corrosion products	



2.4 Local Evolution Rules

In each time increment of the CA model, the center cell will randomly select the target neighbor cells that can react with it and react according to the local rules made. So as to simulate the metal dissolution, product formation and material diffusion processes in the metal corrosion system.

The reactions between different cells in the model include “Transformation” and “Exchange”. Transformation refers to the state change of cells. Exchange refers to the material exchange between the central cell and the target neighbor cell, which can also be interpreted as the location exchange of the cell. The transformation also includes the chemical reaction process of metal dissolution and corrosion products, as well as the permeation process of the corrosive solution cellular S into the void space of the corrosion product cellular L to form compound cellular LS. Due to the tight connection between cell and cell in the CA model in this paper, there are no intercellular spaces. In order to simulate the loose and porous characteristics of metal corrosion products, the form of composite cell is adopted to represent the presence of liquid cell S or D in the void of solid corrosion product cell L. Therefore, the content of reactants in cell S or D is higher than that in composite cell LS or LD, so the chemical reactions of cell S or D are

given priority. The specific local evolution rules of the CA model are shown in Tab. 2. “Cell-1” represents the central cell under each time increment, and “Cell-2” represents the target neighbor cell which acts with “Cell 1”. “T” represents reaction type “Transformation”, and “E” represents reaction type “Exchange”.

Table 2: Local evolution rule

Cell-1	Cell-2	Type	Expression
M	S	T	$M_1 + S_2 \rightarrow D_1 + L_2$
	LS		$M_1 + LS_2 \rightarrow D_1 + LD_2$
B	S	T	$B_1 + S_2 \rightarrow D_1 + L_2$
	LS		$B_1 + LS_2 \rightarrow D_1 + LD_2$
L	S	T	$L_1 + S_2 \rightarrow LS_1 + S_2$
	D		$L_1 + D_2 \rightarrow LS_1 + LS_2$
	LS	E	$L_1 + LS_2 \rightarrow LS_1 + L_2$
	LD		$L_1 + LD_2 \rightarrow LD_1 + L_2$
D	S	T	$D_1 + S_2 \rightarrow L_1 + S_2$
	LS		$D_1 + LS_2 \rightarrow L_1 + LS_2$
LD	S	T	$LD_1 + S_2 \rightarrow L_1 + LS_2$
	LS	E	$LD_1 + LS_2 \rightarrow LS_1 + LD_2$
	D		$LD_1 + D_2 \rightarrow D_1 + LD_2$
LS	D	T	$LS_1 + D_2 \rightarrow LS_1 + L_2$

2.5 Definition of Corrosion Probability

Corrosion rate is often affected by material properties, corrosion environment and other factors. Local corrosion is characterized by inhomogeneity in space. The various pitting morphologies are caused by inhomogeneity in space exactly. Based on the local corrosion model proposed by di Caprio et al. [21], the CA model introduces the parametric definition of corrosion probability in this paper, so as to realize the simulation of different corrosion morphologies.

As shown in Fig. 5, the corrosion probability of Region A and Region B in the crater is different due to their different spatial positions. P_A is used to represent the corrosion probability of Region A, while P_B is used to represent the corrosion probability of Region B. P_A and P_B are functions of the solution probability parameters P and two local parameters λ and ε . The mathematical expressions are as follows:

$$\begin{aligned} P_A &= P\varepsilon(h - h_t) / (h_b - h_t) \leq \lambda \\ P_B &= P(1 - \varepsilon)(h - h_t) / (h_b - h_t) > \lambda \end{aligned} \quad (2)$$

In the expression, h represents the position of the metal cell at a certain moment. h_t and h_b represent the position of the pit mouth and bottom of the pit at that moment, respectively. Dissolution probability P is used to control the total probability that the metal matrix is dissolved in the pitting pit. The value of P is between 0 and 1, depending on the nature of the electrolyte and the activity of the metal. The effect of the spatial parameter λ and the probability parameter ε on the pit morphology is mainly discussed in this paper. Therefore, the value of P is set as 1 by default. The parameter λ divides the pitting pit into two regions with different reaction

probabilities, its value ranges from 0 to 1. The larger the λ is, the larger the proportion of Region A is, and the smaller the proportion of Region B is. Parameter ε is used to adjust the reaction probability in these two regions, and its value ranges from 0 to 1. For the given value, if $(h - h_t) / (h_b - h_t) \leq \lambda$, the central cell is located in the Region A, and the response probability of P_A is $P\varepsilon$. If $(h - h_t) / (h_b - h_t) > \lambda$, the central cell is located in the Region B, the response probability of P_B is $P(1-\varepsilon)$. In summary, the complex simulation of the spatial heterogeneity of local corrosion probability is realized by the introduction of parameters λ and ε .

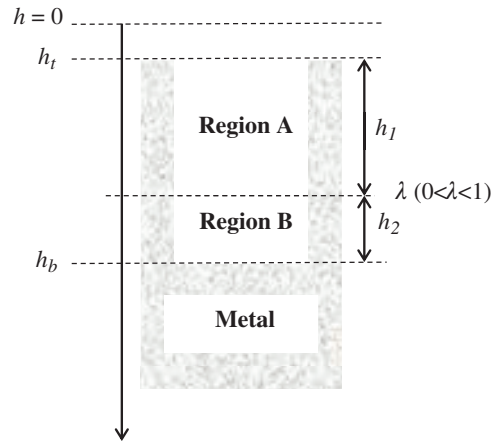


Figure 5: Parametric definition of corrosion probability

3 Result and Discussion

The algorithm for the CA model is written with MATLAB programming software. The evolution of corrosion damage on the surface of steel reinforcement was simulated in the two-dimensional CA space in this paper, and the different corrosion morphology was obtained. The correctness and feasibility of the CA model framework were verified, and the influence of the spatial parameter and the probability parameter on the evolution of corrosion damage was studied.

3.1 Simulation of Different Corrosion Morphologies

The CA model controls the corrosion process by mass loss rate ω , all simulation calculations are terminated at $\omega=5\%$. Due to the complexity of the pitting process, the pitting pits have various morphologies. According to GB/T 18590-2001 [26], the cross-sectional shapes of common metal and alloy pits is shown in Fig. 6. By adjusting the values of λ and ε , the simulation results of different corrosion morphologies can be obtained. The typical pitting corrosion morphologies are shown in Fig. 7, which can correspond to the corrosion morphologies under the specific conditions. Fig. 7a corresponds to Fig. 6a and belongs to the narrow deep pits. Fig. 7b corresponds to Fig. 6b and belongs to the elliptical pits. Fig. 7c corresponds to Fig. 6c and belongs to the subcutaneous pits. Fig. 7d corresponds to Fig. 6f and belongs to the broad-shallow pits. Fig. 7e corresponds to Fig. 6e and belongs to the undercut pits. More importantly, Figs. 7b and 7d match the experimental observations of local corrosion on steel reinforcement surface. The CA model established can evolve according to the set local evolution rules. The simulation results are similar

to the actual corrosion morphologies, which verifies the feasibility of the model in simulating pitting problem of steel reinforcement.

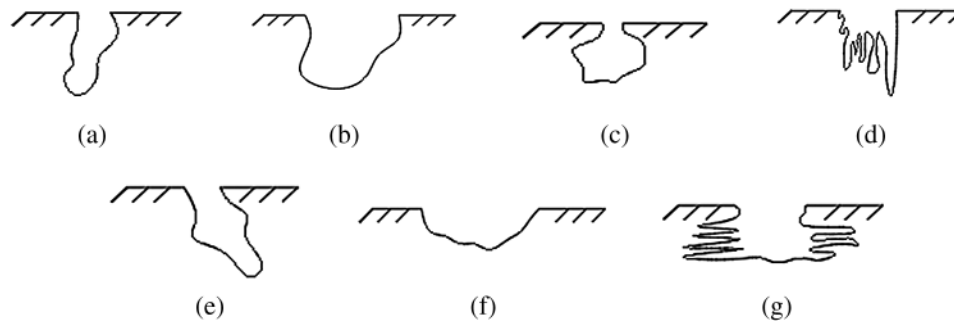


Figure 6: Common corrosion morphology (a) Narrow deep (b) Elliptic (c) Subcutaneous (d) Vertical (e) Undercut (f) Broad-shallow (g) Horizontal

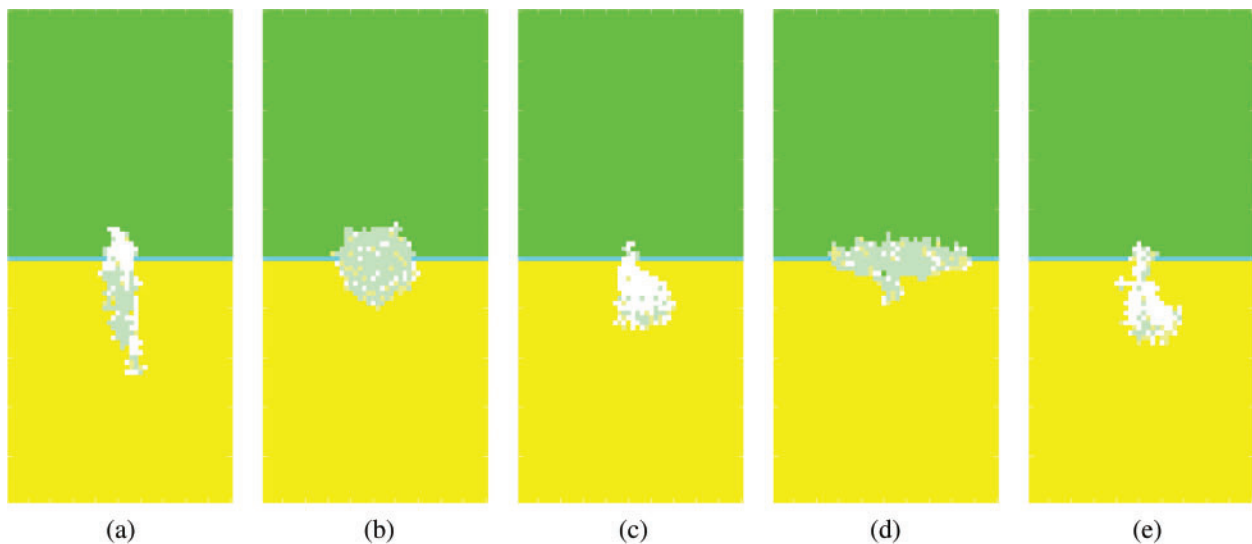


Figure 7: Simulation results of different corrosion morphologies ($\omega = 5\%$) (a) $\lambda = 0.9$, $\varepsilon = 0.1$ (b) $\lambda = 0.6$, $\varepsilon = 0.7$ (c) $\lambda = 0.2$, $\varepsilon = 0.1$ (d) $\lambda = 0.2$, $\varepsilon = 0.9$ (e) $\lambda = 0.6$, $\varepsilon = 0.1$

3.2 Corrosion Evolution of a Single Pit

Fig. 8 shows the transient pattern of corrosion morphology during the corrosion development from the predesigned passive film break when λ and ε are fixed ($\lambda = 0.8$, $\varepsilon = 0.8$). The figure shows the evolution of corrosion morphology and the formation and accumulation of corrosion products. The simulation time T in the figure is a dimensionless quantity, which only represents the number of iterations of the CA program and does not represent the time of actual corrosion experience.

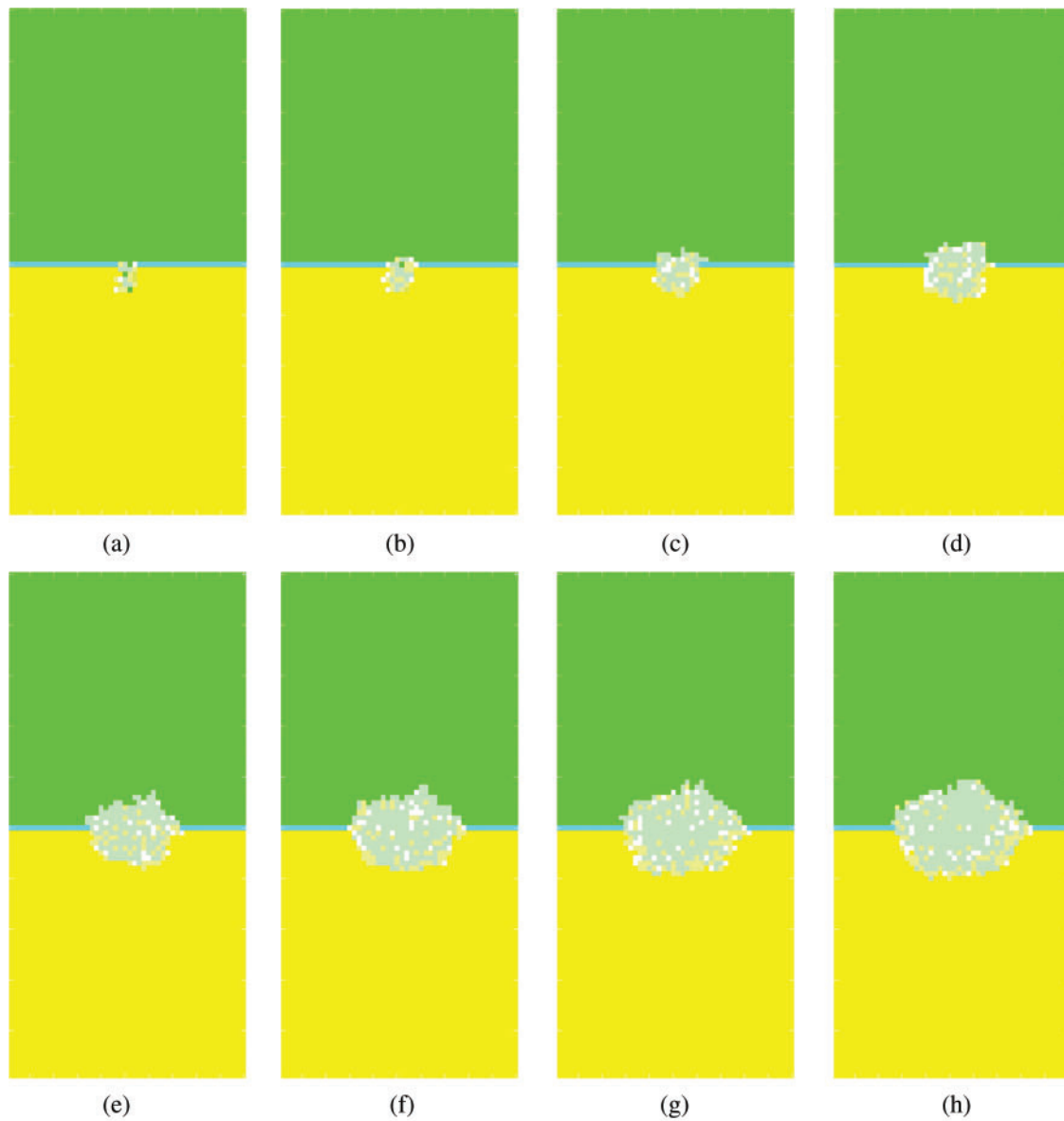


Figure 8: Corrosion evolution of a single pit ($\lambda = 0.8$, $\varepsilon = 0.8$) (a) $T = 5E4$ (b) $T = 1E5$ (c) $T = 2E5$ (d) $T = 3E5$ (e) $T = 4E5$ (f) $T = 5E5$ (g) $T = 5.5E5$ (h) $T = 6E5$

Relevant studies have shown that, the pits are mostly of sharp, narrow and deep shapes in the early stage of corrosion. For example, as shown in Figs. 8a and 8b, the pits are small in the early stage of corrosion, and the accumulation volume of corrosion products is small. Meanwhile, the Corrosive solution cell S contact and react with the metal cell M directly. Since $\lambda = 0.8$ and $\varepsilon = 0.8$, the probability of partial corrosion of Region A, which accounts for 80% of the pit depth, is 0.8. And the probability of partial corrosion of Region B, which accounts for 20% of the pit depth, is 0.2. Therefore, the probability of metal dissolution at the bottom of the pit is small. As the corrosion progresses, the pit develops slowly in depth and rapidly in width. As shown in Fig. 8d, the corrosion pits at this time have developed into spherical, and the accumulation of

corrosion products has reached a degree of number. In the middle and late stage of corrosion, as shown in Figs. 8g and 8h, the width of corrosion pit mouth continues to increase while the depth of corrosion pit changes little. Meanwhile, the shape of corrosion pit has changed from a spherical shape to a long ellipsoid shape. Fig. 9 shows the time-history diagram of the volume expansion rate. As the corrosion process progresses, the ratio of the volume of corrosion products to the volume of dissolved metal is about 2, which meets the expansion amount in test observation.

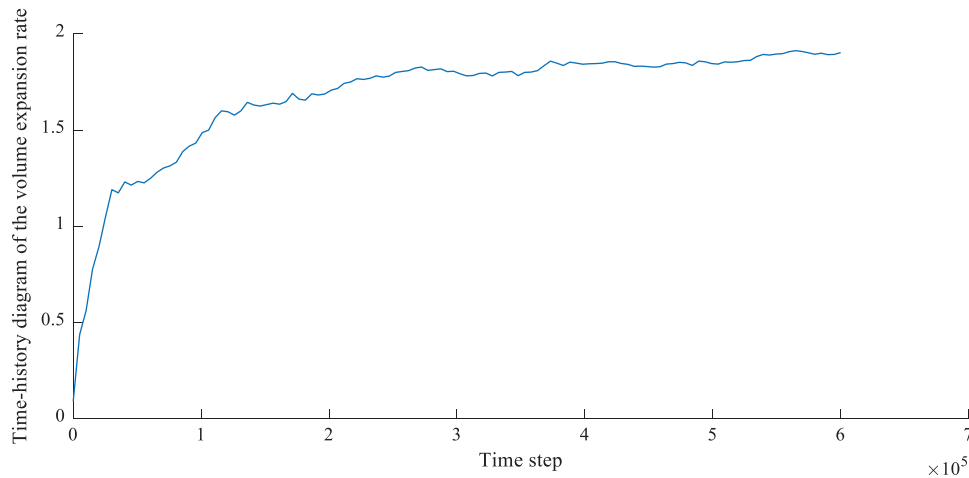


Figure 9: Time-history diagram of the volume expansion rate

Figs. 1a–1d shows several common pit morphologies on the surface of corroded steel reinforcement in concrete. Wang counted 1063 pits on the surface of 40 corroded steel reinforcement [8]. The statistical data of the geometric dimensions (length, width and depth) of the pits were obtained. The length here indicates the size of the pit along the longitudinal side of the reinforcement, and the width indicates the size of the pit along the transverse side of the reinforcement. Through the analysis of relevant data, the aspect ratio (the ratio of length to depth) of the pits of various morphologies was obtained: the aspect ratio of the deep ellipsoid pits shown in Fig. 1a is about 1:1, the aspect ratio of the circular spherical pit shown in Fig. 1b is about 2:1, the aspect ratio of the long ellipsoidal pit shown in Fig. 1c is about 4:1. The groove pit shown in Fig. 1d is further developed from the ellipsoidal pit, with the transverse curvature gradually becoming zero and the transverse boundary gradually becoming indistinct, and finally developing into the groove pit. It can be observed from Fig. 8 that the whole change process of steel pitting pits from the initial narrow and deep type to the spherical shape and then to the long ellipsoid shape basically conforms to the experimental research conclusion, which indicates that the CA model established can realize the simulation of steel reinforcement corrosion in concrete.

Studies have shown that the development of corrosion pit depth exists a critical value [9]. As the corrosion progresses, the corrosion products accumulate more and more closely at the pit mouth, which prevents the corrosion solution from entering the bottom of the pit. In addition, the area around the pit mouth begins to activate, and more new pitting points appear. As a result, the potential difference between the inside and outside of the pit decreases, which slows down the development of the pit depth and increases the aspect ratio of the pit. Two-dimensional CA has no concept of pit width, but length and depth. It can be seen from Fig. 8 that, the depth of the pit changes less and less with the progress of corrosion, and it is almost unchanged at last.

Fig. 10 shows the time history of the number of dissolved metal cells when λ and ε are constant ($\lambda = 0.8$, $\varepsilon = 0.8$). The metal cells contact fewer corrosive cells due to the small pit area at the initial stage of corrosion, and the corrosion rate is low. As the corrosion progresses, the corrosion pit area increases, and the dissolution rate of metal cells increases gradually. The corrosion rate remained unchanged in the middle and late stage. According to Figs. 8 and 10, when the growth rate of dissolved metal cells is basically unchanged, the growth rate of pit depth decreases, and the development of pit length gradually accelerates, which is consistent with the existing research conclusions.

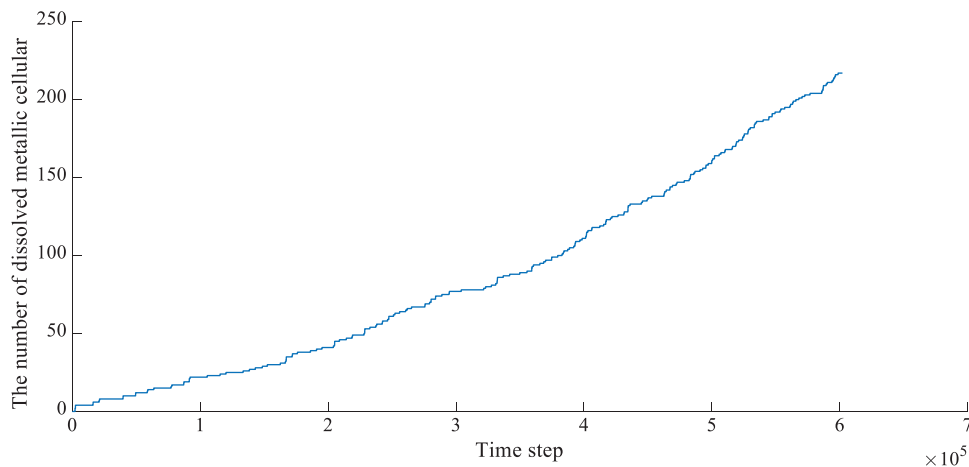


Figure 10: Time-history diagram of the number of dissolved metal cells

3.3 The Effect of the Parameter λ on Corrosion Morphology

Steel reinforcement pitting is spatially non-uniform. According to Fig. 5, the local corrosion space parameter λ represents the ratio of the depth of Region A to the total depth of the pitting at different time steps. During a full run of the program, λ is always constant. As the pitting evolves constantly, the maximum depth of the pit may be different at different time steps, and the depth of Region A will also change accordingly. Fig. 11 shows the corrosion morphologies under different λ values when $\varepsilon = 0.1$ and $\omega = 5\%$. As shown in Fig. 11a, the parameter λ is 0.1, indicating that the depth of Region A in the pitting accounts for 10% of the total pit depth. When the parameter ε is 0.1, the probability of corrosion in Region A is 0.1, and the probability of corrosion in Region B is 0.9. Meanwhile, the probability of corrosion reaction in Region A with the small proportion is also small, and that in Region B with a large proportion is also large. Therefore, the degree of corrosion in Region A is relatively light, while the degree of corrosion in Region B is relatively serious. The corrosion morphology corresponds to the subcutaneous type of corrosion pits as shown in Fig. 6c. The simulation results of the corrosion morphology are consistent with the theoretical analysis, and all the morphologies in Fig. 11 conform to the above analysis logic.

And it can be seen from Fig. 11: When the parameter ε remains unchanged, as λ increases from 0.1 to 0.9 step by step, the proportion of Region A with low corrosion probability increases gradually, while the proportion of Region B with high corrosion probability decreases gradually. With the occurrence of corrosion at the bottom of the corrosion pit and the increase of the depth of the corrosion pit, part of the Region B gradually changes into the Region A, which makes it

difficult for the corrosion pit to expand in the direction of length and continue to develop in the direction of depth. The corrosion morphology gradually evolved into the narrow and deep type.

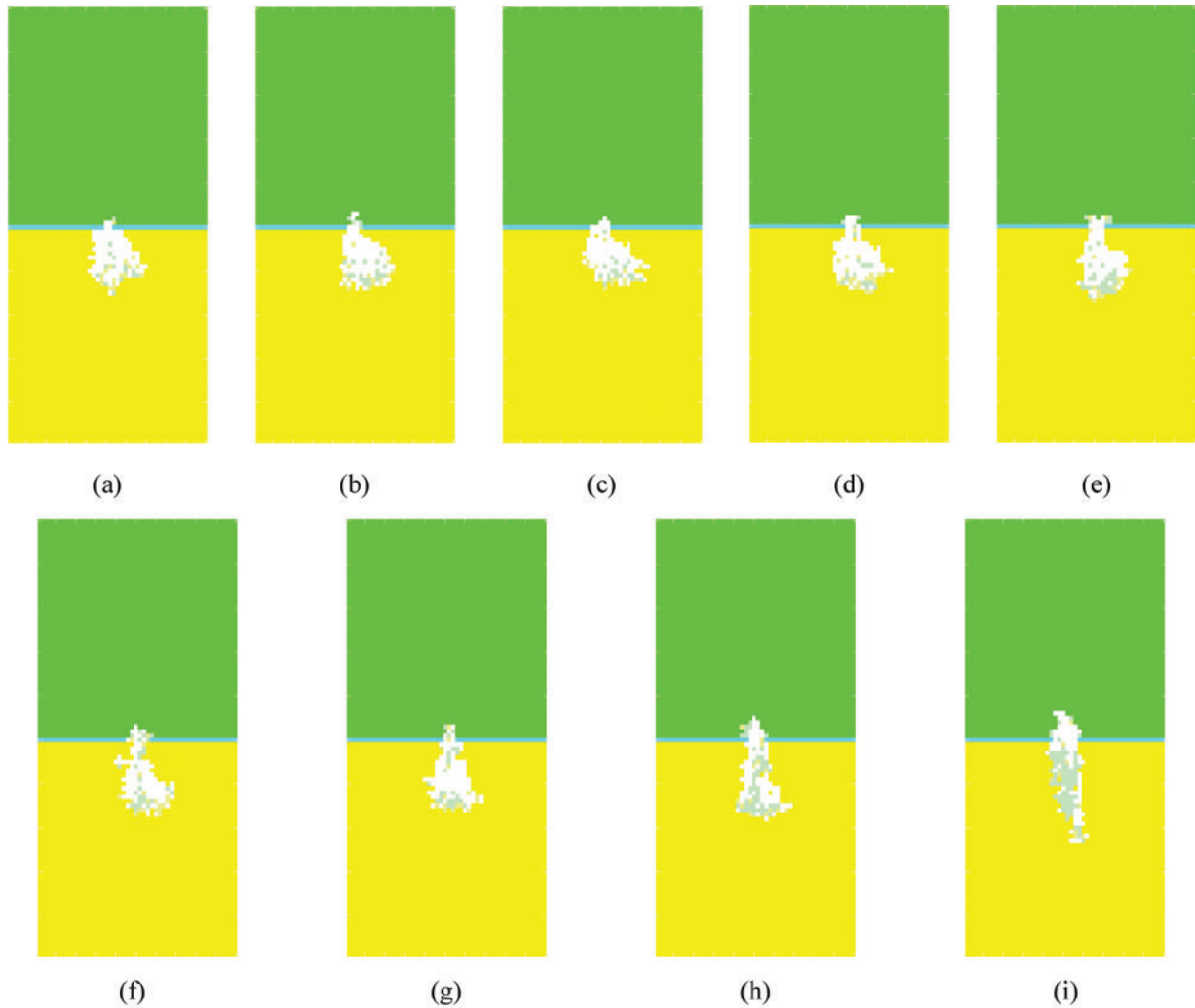


Figure 11: The effect of λ on corrosion morphology ($\varepsilon = 0.1$, $\omega = 5\%$) (a) $\lambda = 0.1$ (b) $\lambda = 0.2$ (c) $\lambda = 0.3$ (d) $\lambda = 0.4$ (e) $\lambda = 0.5$ (f) $\lambda = 0.6$ (g) $\lambda = 0.7$ (h) $\lambda = 0.8$ (i) $\lambda = 0.9$

3.4 The Effect of the Parameter ε on Corrosion Morphology

The local corrosion probability parameter ε represents the corrosion probability of the metal cell in Region A, and the probability of corrosion in Region A is generally different from that in Region B (except $\varepsilon = 0.5$). Different corrosion morphologies can be obtained by adjusting the ε value. Fig. 12 shows the corrosion morphologies when $\lambda = 0.6$ and $\omega = 5\%$, so as to explore the effect of ε value on the corrosion morphology.

As shown in Fig. 12a, the parameter $\lambda = 0.6$ indicates that the depth of Region A occupies 60% of the total depth. The parameter ε is 0.1, so the corrosion probability of Region A is 0.1,

and the corrosion probability of Region B is 0.9. Meanwhile, Region A with the large proportion in the corrosion pit is less likely to be corroded, and Region B with the small proportion is more likely to be corroded. Therefore, Region A in the upper part of the pit is less corroded, while area B in the lower part is more corroded. The whole corrosion morphology is subcutaneous as shown in Fig. 6c. This analysis is applicable to each subgraph in Fig. 12. Thus, we can draw the following conclusions: When the parameter λ remains the same, as the ε increased from 0.1 to 0.9 step by step, the corrosion probability of Region A, which accounts for a large proportion of the whole pit, increases gradually. The corrosion probability of Region B with a relatively small proportion decreases gradually, which results in the pit gradually changes from subcutaneous type to narrow and deep type, then to spherical type with severe upper corrosion, and finally to wide and shallow type. This process accords with the law of corrosion pit development of corroded reinforcement.

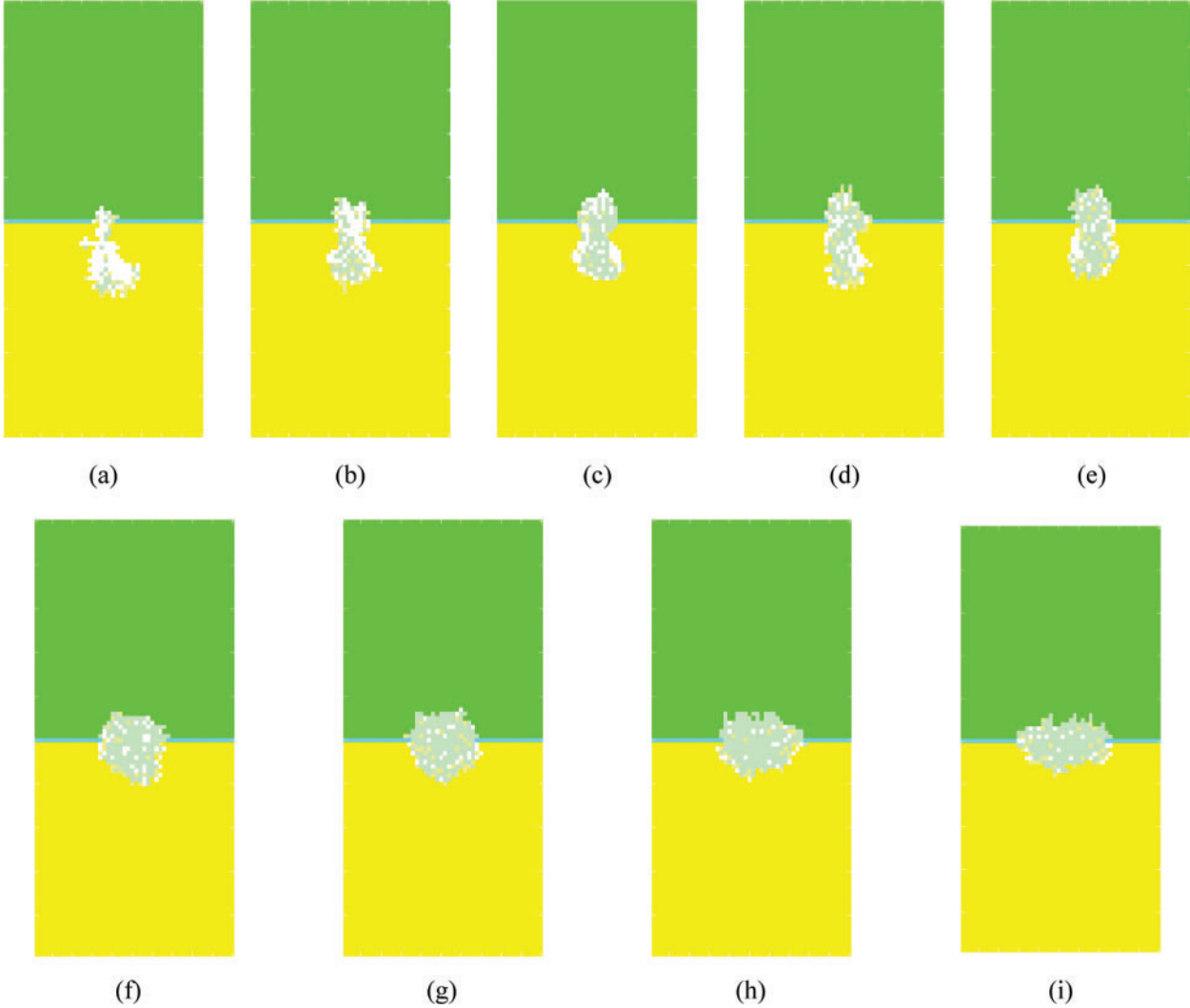


Figure 12: The effect of ε on corrosion morphology ($\lambda = 0.6, \omega = 5\%$) (a) $\varepsilon = 0.1$ (b) $\varepsilon = 0.2$ (c) $\varepsilon = 0.3$ (d) $\varepsilon = 0.4$ (e) $\varepsilon = 0.5$ (f) $\varepsilon = 0.6$ (g) $\varepsilon = 0.7$ (h) $\varepsilon = 0.8$ (i) $\varepsilon = 0.9$

4 Conclusions

(1) By changing the values of local parameters λ and ε in the CA model, the simulation results of various corrosion morphologies can be obtained, corresponding to the cross-sectional shapes of common metal and alloy pits in GB/T 18590-2001. The CA model in this paper can realize the simulation of complex metal pitting process.

(2) As the corrosion progresses, the corrosion pit expands continuously both laterally and longitudinally, the damage degree of the passive film on the surface of reinforcement becomes more and more serious. The corrosion products gradually increase and accumulate in the pit mouth. When the parameters $\lambda = 0.8$ and $\varepsilon = 0.8$, the typical spherical pit on the surface of corroded steel reinforcement in concrete is obtained. The ratio of the volume of corrosion products to the volume of dissolved metal is about 2. The simulation results are consistent with the relevant experimental results.

(3) The parameter λ divides the corrosion space into two regions with different proportions. When $\varepsilon = 0.1$, with the increase of λ , the proportion of the regions with less corrosion probability to the whole pit increases gradually, which leads to the continuous development of corrosion towards depth. The parameter ε indicates the probability of corrosion in the upper region. When $\lambda = 0.6$, with the increase of ε , the probability of corrosion in the upper region increases gradually. The corrosion morphology changes from subcutaneous to narrow and deep, then to more severely corroded spherical, and finally to wide and shallow.

Funding Statement: The works described in this paper are substantially supported by the grant from National Natural Science Foundation of China (Grant No. 51678135); Natural Science Foundation of Jiangsu Province (No. BK20171350); Six Talent Peak Projects in Jiangsu Province (JNHB-007), which are gratefully acknowledged.

Conflicts of Interest: The authors declare that they have no conflicts of interest to report regarding the present study.

References

1. Alan, P., Crane (1983). *Corrosion of reinforcement in concrete construction*. Published for the Society of Chemical Industry, London: Ellis Horwood, Halsted Press.
2. Jia, H., Yan, G., Yan, G. (2005). Study on corrosion of reinforcement in concrete. *China Safety Science Journal*, 15(5), 56–59. DOI 10.16265/j.cnki.issn1003-3033.2005.05.013.
3. Qin, Z. (2018). *Study on coupling analysis method of chloride erosion and steel corrosion expansion in reinforced concrete (Ph.D. Thesis)*. Nanjing: Southeast University.
4. Val, D. V., Melchers, R. E. (1997). Reliability of deteriorating RC slab bridges. *Journal of Structural Engineering*, 123(12), 1638–1644. DOI 10.1061/(ASCE)0733-9445(1997)123:12(1638).
5. Stewart, M. G. (2009). Mechanical behaviour of pitting corrosion of flexural and shear reinforcement and its effect on structural reliability of corroding RC beams. *Structural Safety*, 31(1), 19–30. DOI 10.1016/j.strusafe.2007.12.001.
6. Stewart, M. G., Al-Harthy, A. (2008). Pitting corrosion and structural reliability of corroding RC structures: Experimental data and probabilistic analysis. *Reliability Engineering & System Safety*, 93(3), 373–382. DOI 10.1016/j.ress.2006.12.013.
7. Shen, D., Wu, S. (2004). Research on corroded rebar performance and corrosion model test in concrete in atmospheric environment. *China Concrete and Cement Products*, 3, 46–50. DOI 10.19761/j.1000-4637.2004.03.014.

8. Wang, B., Yuan, Y. S., Chen, R. (2011). The character and evolution of corrosion pits on steel reinforcing bar surfaces corroded by chloride. *Journal of China University of Mining & Technology*, 40(2), 240–245. DOI CNKI:SUN:ZGKD.0.2011-02-014.
9. Wang, B. (2012). *Failure mechanism and degradation model of RC structure corroded by chloride attack (Ph.D. Thesis)*. Xuzhou: China University of Mining and Technology.
10. Xu, X. (2020). *Experimental study on the concrete cracking behavior due to rebar non-uniform corrosion (Ph.D. Thesis)*. Hangzhou: Zhejiang University.
11. Wang, X., Zhang, W., Gu, X., Dai, H. (2013). Determination of residual cross-sectional areas of corroded bars in reinforced concrete structures using easy-to-measure variables. *Construction and Building Materials*, 38(1), 846–853. DOI 10.1016/j.conbuildmat.2012.09.060.
12. He, L. R., Yin, Z. P., Huang, Q. Q., Liu, J. P. (2015). Simulation of local corrosion on metal surface with CA method. *Journal of Aeronautical Materials*, 35(2), 54–63. DOI CNKI:SUN:HKCB.0.2015-02-007.
13. Cordoba-Torres, P., Nogueira, R., de Miranda, L., Brenig, L., Wallenborn, J. et al. (2001). Cellular automaton simulation of a simple corrosion mechanism: mesoscopic heterogeneity versus macroscopic homogeneity. *Electrochimica Acta*, 46(19), 2975–2989. DOI 10.1016/S0013-4686(01)00524-2.
14. Malki, B., Baroux, B. (2005). Computer simulation of the corrosion pit growth. *Corrosion Science*, 47(1), 171–182. DOI 10.1016/j.corsci.2004.05.004.
15. Bartosik, Ł., di Caprio, D., Stafiej, J. (2012). Cellular automata approach to corrosion and passivity phenomena. *Pure and Applied Chemistry*, 85(1), 247–256. DOI 10.1351/PAC-CON-12-02-01.
16. Pidaparti, R. M., Palakal, M. J., Fang, L. (2005). Cellular automata approach to aircraft corrosion growth. *International Journal on Artificial Intelligence Tools*, 2(14), 361–369. DOI 10.1142/S0218213005002144.
17. Stafiej, J., di Caprio, D., Bartosik, Ł. (2013). Corrosion-passivation processes in a cellular automata based simulation study. *The Journal of Supercomputing*, 65(2), 697–709. DOI 10.1007/s11227-013-0933-8.
18. Li, L., Li, X., Xiao, K., Dong, C. (2010). Cellular automata simulation on the early stages of metal corrosion in moist atmospheric environment. *Journal of Chinese Society for Corrosion and Protection*, 30(2), 114–118. DOI CNKI:SUN:ZGFF.0.2010-02-006.
19. Wang, H., Lv, G. Z., Zhang, Y. H. (2008). Cellular automation simulations of corrosion pit growth. *Corrosion Science and Protection Technology*, 20(6), 472–475. DOI 10.3969/j.issn.1002-6495.2008.06.021.
20. Liu, P. (2011). *Microscale simulation of corrosion damage evolution of metals (Ph.D. Thesis)*. Yinchuan: Ningxia University.
21. di Caprio, D., Vautrin-UI, C., Stafiej, J., Saunier, J., Chaussé, A. et al. (2011). Morphology of corroded surfaces: Contribution of cellular automaton modelling. *Corrosion Science*, 53(1), 418–425. DOI 10.1016/j.corsci.2010.09.052.
22. Molina, F. J., Alonso, C., Andrade, C. (1993). Cover cracking as a function of rebar corrosion: Part 2—Numerical model. *Materials and Structures*, 26(9), 532–548. DOI 10.1007/BF02472864.
23. Ji, Y., Yuan, Y., Song, M., Shen, J., Xu, C. (2011). Volume expansion characteristic and mechanism of rebar corrosion products in concrete with different corrosion approaches. *Journal of Beijing University of Technology*, 37(11), 1677–1683. DOI CNKI:SUN:BJGD.0.2011-11-013.
24. Guo, D., Ren, K., Wang, Y., Guo, X., Zhang, E. (2014). Three-dimensional cellular automata model for predicting local corrosion. *Mechanics in Engineering*, 36(4), 447–452. DOI 10.6052/1000-0879-13-495.
25. Yuan, Y., Ji, Y. S., Mou, Y. J. (2007). Propagation and model of distribution for corrosion of steel bars in concrete. *China Civil Engineering Journal*, 7, 5–10. DOI JournalArticle/5aeac91c095d70944f882f5.
26. Institute Central Iron Steel Research (2001). Corrosion of metals and alloys-evaluation of pitting corrosion (GB/T 18590-2001). General Administration of Quality Supervision, Inspection and Quarantine of the People's Republic of China.